Available online at www.sciencedirect.com

ScienceDirect

Physics Procedia 12 (2011) 353–363

Physics Procedia

Corrosion and wear resistance improvement of magnesium alloys by laser cladding with Al-Si.

Bernabe Carcel[a]*, Jesus Sampedro[a], Ana Ruescas[b], Xavier Toneu[b]

[a]AIDO, C/ Nicolas Copernico 7, 9 y 11. Paterna 46980, Spain

[b]Aleaciones estampadas AESA, Camino del Bony S/N, Catarroja 46470, Spain

Abstract

Laser cladding with Al-Si powders have been carried out on three different magnesium alloys (AZ61, ZK30 and WE54) in order to improve their wear and corrosion properties using Nd:YAG CW laser. Optimized parameters allow obtaining crack and pore free coatings with good metallurgical bonding. Special care in shielding atmosphere is required to avoid porosity and corrosion. The hardness of the coatings is higher (130-250 HV) than that of as-received alloys. Salt spray corrosion tests and pin on disc sliding wear tests were carried out confirming that Al-Si coatings improves the wear and corrosion resistance of the alloys.

Keywords: laser cladding; magnesium; corrosion; wear; AlSi

1. Introduction

The continuous demand of lightweight materials in the automotive and aerospace industries has made of magnesium alloys one of the most attractive materials, due to their high specific strength and low density (from 1.74 to 1.85 g cm-3). Besides, magnesium alloys have good castability, hot formability and recyclability, excellent machinability and sound damping capabilities. Nevertheless magnesium alloys have a number of undesirable properties, namely, limited strength, fatigue and creep resistance at elevated temperatures, low stiffness and limited ductility. Moreover magnesium alloys show poor surface properties such as high chemical reactivity, low hardness, corrosion resistance and wear properties, which limit their extensive use in some applications.

Surface modification by laser technology seems a suitable solution to avoid these surface related drawbacks without affecting the bulk properties of the material. Up to now, different approaches have been explored in the field of laser cladding on magnesium alloys, Wang et al. [1] investigated the laser cladding of homogeneous coating onto magnesium alloys. Nevertheless, the great majority of studies were focused on laser cladding with heterogeneous coating materials, most of them based on Al-base alloys and Al-base metal matrix composites [2, 3], concluding that Al as alloying element could enhance the corrosion resistance giving at the same time good bonding properties to the interface. It is important to notice that magnesium is a very active metal, and that melted magnesium can react with common metals and gases (oxygen, nitrogen) to form intermetallic compounds and oxides [4]. Therefore,

* Corresponding author. Tel.: +34-961-318-051; Fax: +34-961-318-007.
E-mail address: bcarcel@aido.es

doi:10.1016/j.phpro.2011.03.045

melting of magnesium may cause deterioration of the alloys. In this way, special care is necessary during the laser cladding, particularly in optimizing the shielding gas protection.

In the present study, an attempt has been made to improve wear and corrosion resistance of the following magnesium alloys families: AZ61, ZK30 and WE54 by laser surface cladding with Al-Si powders. A wide parameterization of the cladding conditions and a detailed characterization of the laser processed zone have been carried out, including hardness measurement of the laser cladding Al-Si layers, evaluation of corrosion performance (salt spray test) and evaluation of the sliding wear properties (pin on disc test). The results show that this technique allows achieving defect free coatings with improved hardness, corrosion and wearing behaviour of the magnesium alloys.

2. Experimental methods

2.1. Material and specimen preparation

Magnesium alloy substrates directly cut from extruded bars of AZ61, ZK30 and WE54 were used as target for laser cladding. Prior to laser treatment, the specimens were ground with emery paper up to 600 grit so as to obtain uniform surface conditions. After ground, the substrate was cleaned in acetone to remove soils or greases on the surface of the samples.

The composition of the three magnesium alloys used as base materials in this study is listed in table 1.

Table 1. Composition of magnesium base materials

	%Mg	*%Al*	*%Zn*	*%Si*	*%Cu*	*%Mn*	*%Fe*	*%Ni*	*%Zr*	*%Y*	*%Nd*	*%Factored HRE+Nd*
AZ61	Bal.	6.275	0.542	0.044	<0.001	0.318	0.003	<0.001	-	-	-	-
WE54	Bal.	-	-	<0.01	<0.01	0.01	0.001	<0.001	0.52	5.1	1.8	2.8
ZK30	Bal.	<0.001	3.206	<0.01	<0.001	0.001	0.002	<0.001	0.324	-	-	-

For the laser cladding process, commercial aluminium / silicon alloy powder (Sulzer Metco 52-CNS) with particle size +45-90μm. was used. Powder composition is shown is table 2.

Table 2. Composition of AlSi powder

	%Al	*%Si*	*%Fe*	*%Mn*	*%Cu*
METCO 52CNS	Bal.	11.8	0.17	<0.01	0.01

2.2. Laser cladding

Laser cladding experiments were carried out by means of a Nd:YAG laser (wavelength 1064 nm) TRUMPF model HL1006D, with maximum output power of 1kW at the work piece. The beam is conveyed to a lens assembly of focal length 200 mm within a coaxial deposition head via an optical fibre with internal diameter 0.6 mm. This focused the beam to a circular spot with diameter 1.5 mm. and nominally Gaussian beam profile at the deposition point, which was positioned 8 mm beyond the end of the nozzle. The powder was delivered by a Sulzer Metco Twin 10C accurate powder feeder. Coaxial powder injection nozzle was used. Shielding gas control is integrated in the nozzle coaxially to the laser beam. Relative motion between nozzle and substrate is done by X-Y-Z motion table controlled by CNC (figure 1).

Processing parameters have been evaluated for each material in order to obtain good coatings with little or no defects in terms of porosity and cracking. In this sense, reduced speed (100 mm/min) was set for all the coatings, after verifying that reduced speed helps avoiding porosity. Laser power was optimized to 240 W for AZ61 substrate, 340 for ZK30 and 210W for WE54.

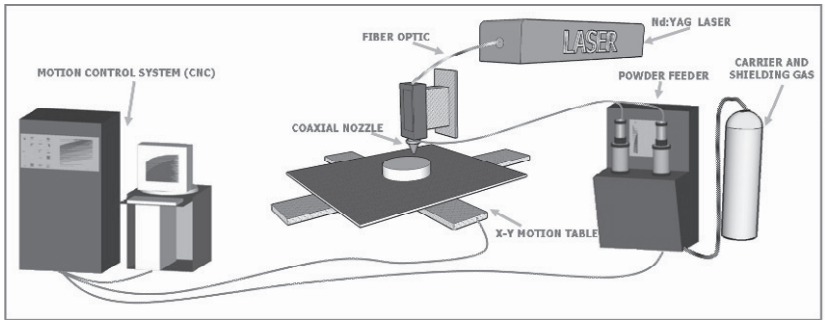

Figure 1. Scheme of laser cladding station.

Good shielding is important to avoid burning or porosity and protect the optics from metal slag (cinders). The shielding gas also influences the formation of plasma. Helium, with a high ionization potential of 24.5 eV and with good thermal conductivity, has a high plasma formation threshold [4]. Thus, helium was used as shielding gas, with a flow rate of 25 lpm. in order to minimize plasma formation. Helium as well was used as carrier gas with a volume flow of 3 lpm.

Once the optimum processing parameters were set for each magnesium substrate, 9 samples (3 from each alloy) with a coating surface (35x35 mm) were processed by laser cladding using an overlapping of 40%. A set of samples (3) was used for salt spray corrosion testing, another set for microhardness testing and metallography, and the last one for sliding wear (pin on disc) testing.

2.3. Geometry and microstructure analysis.

In order to analyze the geometry, structure and flaws of deposited coatings, resulting samples were prepared for metallographic characterization. Firstly, samples were cut transversely to the laser track by a Jeanwirth cuto-20 cutting wheel, after cutting, the samples were hot mounted (Struers labopress-3) and finally grinded (mesh 120 – 1000) and polished with diamond paste to 1 μm. (Jeanwirth TG 200/1). After that, samples were cleaned with ethanol and dried in hot air. Metallographic samples were then inspected by light microscopy (Nikon optiphot-M) , scanning electron microscope (SEM) and energy dispersive X-ray spectrometer (EDS) by using a Jeol JSM6300 and JSM5410. SEM results were analysed with INCA software from Oxford Instruments.

2.4. Microhardness testing.

The microhardness was evaluated by using a Struers Duramin microhardness tester with Vickers indenter. Cross sections of the samples were cut transversely to the cladding direction. Micro Vickers indenter was used, loaded at 200 g. with a loading time of 10 s (HV0.2/10). Different places at the surface where measured in order to obtain a microhardness profile from the substrate material to the coating. Average microhardness was obtained in singular areas from at least 3 measurements.

2.5. Salt spray corrosion testing.

Salt spray tests were carried out following the standard ISO 9227:2006. Surface preparation of corrosion test samples consisted of initial surface machining to flatness with a milling machine, grinding by 220, 600 and 1000 SiC papers, and then polishing with 3 μm diamond powder slurry. Polished surfaces were cleaned in an ethanol solution. For testing, samples were sprayed with NaCl dissolution (50 g/l) inside a salt spray chamber. For this test 6 samples were used, 3 base material samples (AZ61, ZK30 and WE54) and 3 laser cladding coated samples (Al-Si on AZ61, Al-Si on ZK30 and Al-Si on WE54). The surface of the samples was checked every 24 hours until severe corrosion was observed.

2.6. Sliding wear testing (pin o disc).

The sliding wear tests were carried out with a pin on disc tester Microtest MT2/60/SCM/T. No lubricant was used for the tests. The counter-face pin was made of silicon nitride Si3N4 (1600 HV) with a diameter of 4 mm. Test configuration consisted in a sliding velocity of 0.16 m/s with a load of 2 N. The sliding distance was 100 to 500 m. The width of wear scars was measured by an optical microscope. Volumetric wear loss was estimated from the track width, calculating the section area (function of the track width and pin diameter) and multiplying it by the track length (function of the track diameter). Volumetric wear rates were calculated by dividing the volumetric loss by the sliding distance.

Compositions, morphologies and microstructures of worn surfaces and wear debris were characterized by scanning electron microscope (SEM) and energy dispersive X-ray spectrometer (EDS).

3. Results and discussion

3.1. Microstructure of the laser cladding coatings.

3.1.1. Al-Si on AZ61 Mg alloy

Light microscopy analysis showed good metallurgical bonding and lack of defects like pores and cracks. The rise in the melting layers dilution for subsequent tracks is related with the laser absorption increase as the substrate heats up (figure 2).

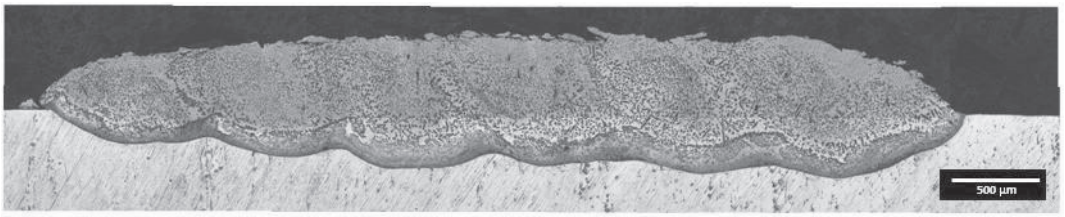

Figure 2. Cross section microstructure of AZ61 laser cladding coating.

The average thickness of the melting layer is 0.65 mm. Three different areas are identified in the coating. The interface area is characterized by a eutectic microstructure surrounded by big acicular particles (figure 3). In the middle, the microstructure contains smaller acicular particles surrounded by a fine dendritic matrix. The upper area of the coating shows a biphasic microstructure.

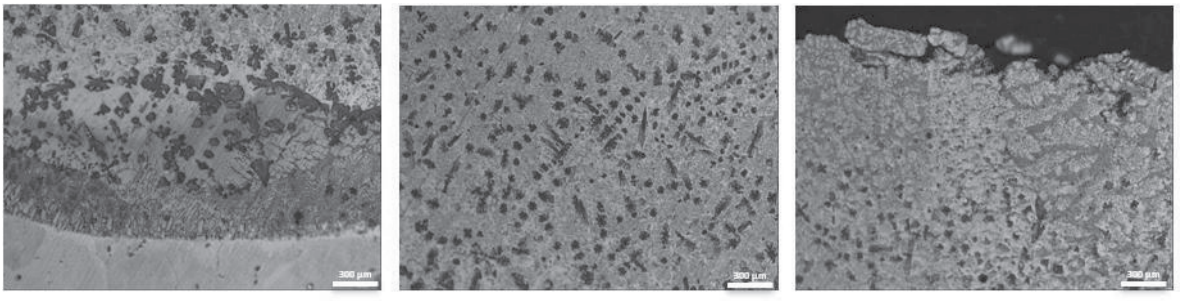

Figure 3. Microstructure details. Left: Interface; Middle: Medium area; Right: Top area.

The corresponding EDS analysis shown in figure 4 gives the element distribution along the labeled line, crossing from the substrate (bottom part) to the melting zone (top). In terms of element composition, the melting zone is divided into two clearly distinct areas separated by a band of intermetallic particles formed during the laser cladding process. The bottom area, close to the substrate is characterized by having a big amount of Mg (~65 %), with lower Al content (~28%). In the upper area the Al content of the matrix raises to ~94.5 % with ~2.1% of Mg and ~3.3% of Si. The same morphological tendency, with little variations, has been observed for the coatings on ZK30 and WE54 Mg alloys.

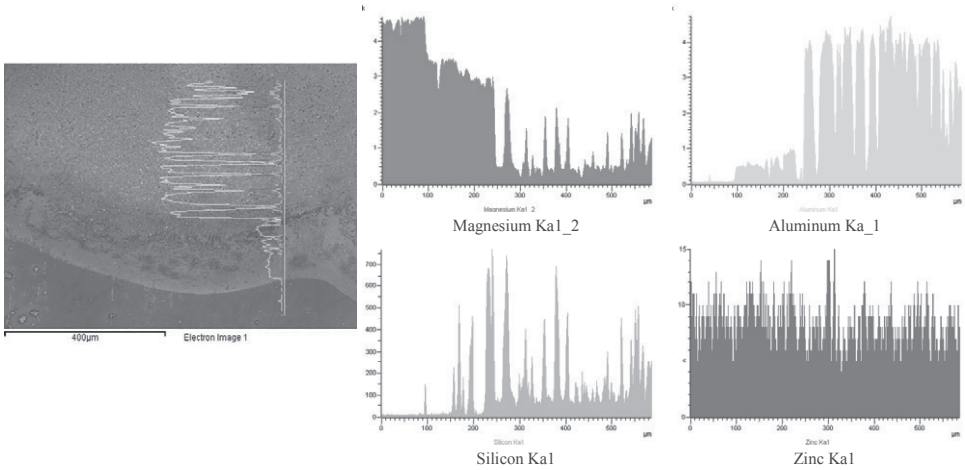

Figure 4. Scanning electron micrograph of Al-Si coating on AZ61 Alloy. Elements distribution along the labeled line.

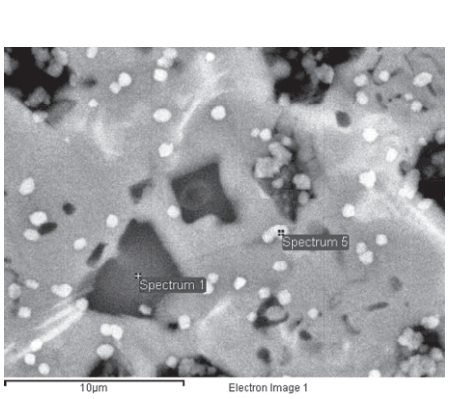

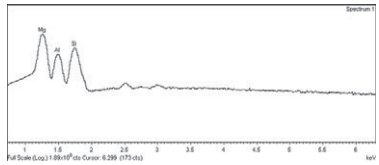

Spectrum 1. Black particles

Element	Weight%	Atomic%
Mg K	53.60	56.84
Al K	15.00	14.34
Si K	31.40	28.83
Totals	100.00	

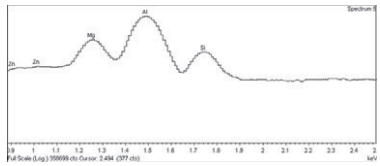

Spectrum 5. White particles

Element	Weight%	Atomic%
Mg K	7.44	8.23
Al K	83.79	83.50
Si K	8.54	8.18
Zn K	0.23	0.10
Totals	100.00	

Figure 5. Scanning electron micrograph and spectrum (EDX) of intermetallic particles in the melting zone of Al-Si coating on AZ61 Alloy.

Two kind of intermetallic particles have been analyzed in the melting zone. Figure 5 depicts the composition of these particles from EDX analysis. Black particles are distributed in the lower and medium part of the melting zone, forming as well a band between the lower zone and the rest of the coating. White particles are homogenously distributed in the medium and upper area of the melting zone.

3.1.2. Al-Si on ZK30 Mg alloy

Figure 6 shows the cross section of Al-Si coating on ZK30 alloy. The coating is free of pores and cracks with good metallurgical bonding.

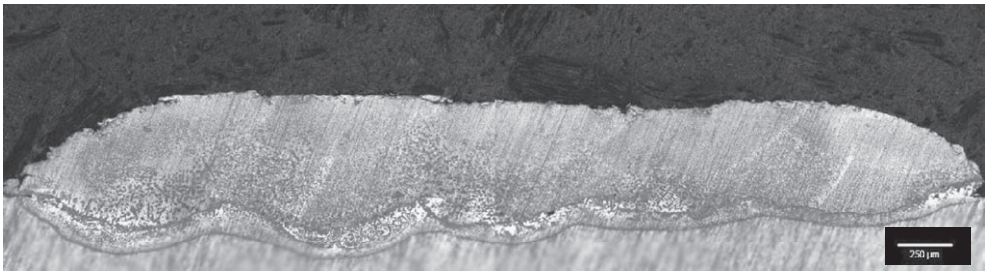

Figure 6. Cross section microstructure of ZK30 laser cladding coating.

The EDX elements distribution along the labelled line from the substrate to the melting zone is shown in figure 7.

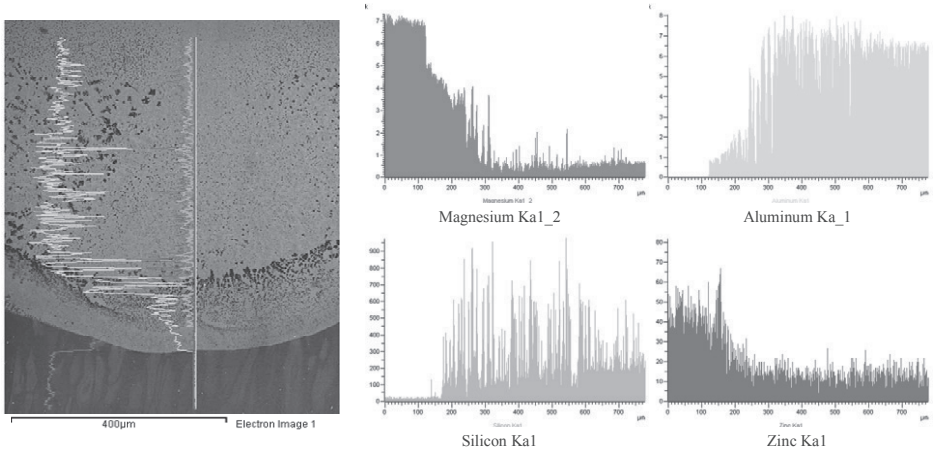

Figure 7. Scanning electron micrograph of Al-Si coating on ZK30 Alloy. Elements distribution along the labeled line.

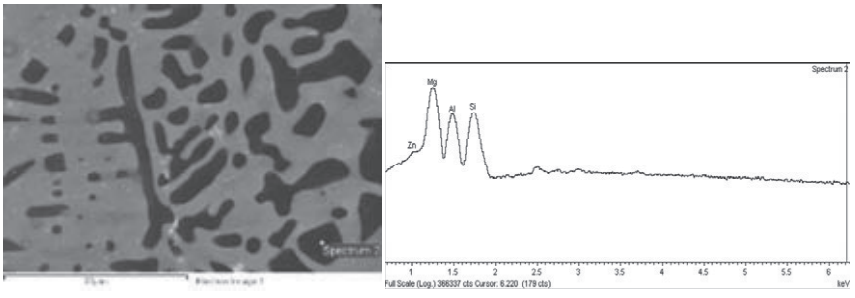

Element	Weight%	Atomic%
Mg K	51.15	54.44
Al K	21.02	20.15
Si K	27.39	25.23
Zn K	0.44	0.18
Totals	100.00	

Figure 8. Scanning electron micrograph and spectrum (EDX) of intermetallic dark particles found in Al-Si coating on ZK30 Mg. alloy.

There is, as observed for the AZ61 alloy, two clearly different areas in the melting zone. The lower part, close to the substrate is separated from the upper part by a band of dark intermetallics. This lower part is rich in substrate elements Mg (~67.45%) and Zn (~3.06%), with increasing content of Al (~28.9%). The upper part is rich in Al (~75%) and Si (~12%) with lower Mg content (~8.5%). Dark intermetallic particles composition (figure 8) is quite similar to those found for AZ61 alloys, probably sharing the same stoichiometry.

3.1.3. Al-Si on WE54 Mg alloy

Al-Si coatings on WE54 Mg alloy have a microstructure very similar to the previously analyzed AZ61 and ZK30 alloys (figure 9).

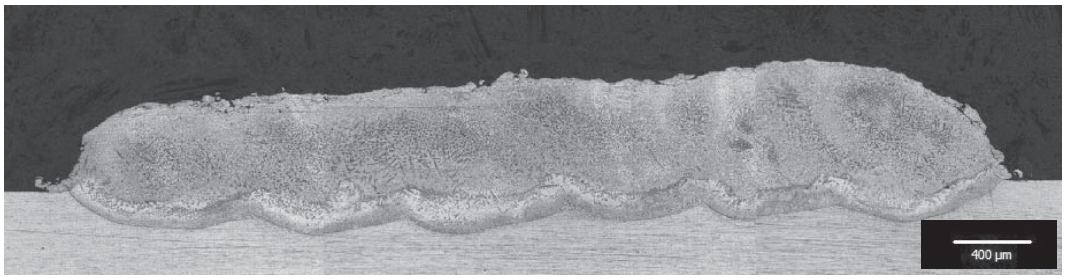

Figure 9. Cross section microstructure of WE54 laser cladding coating.

EDX analysis shows the element composition along the labeled line (figure 10), from the substrate to the melting zone.

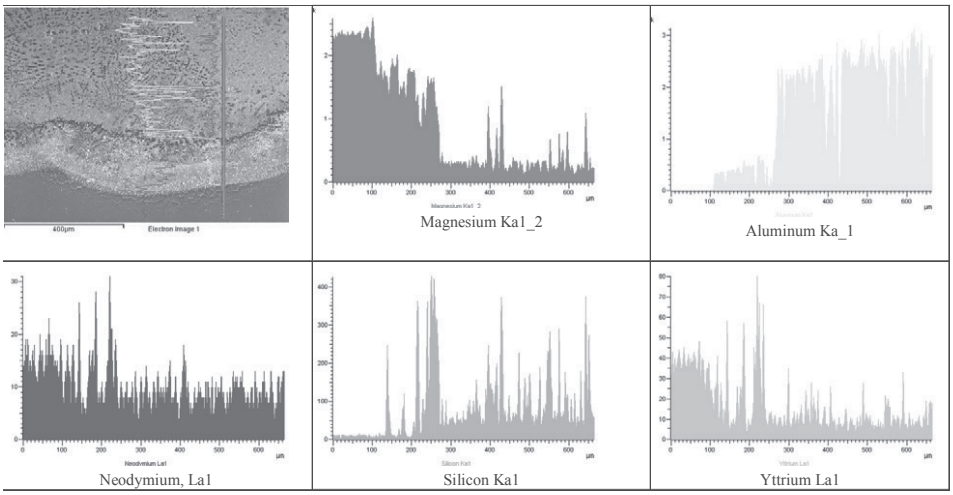

Figure 10. Scanning electron micrograph of Al-Si coating on WE54 Alloy. Elements distribution along the labeled line.

As for the AZ61 and ZK30 alloys, two different areas separated by a band of intermetallics are clearly identifiable. As before, the lower part is rich in Mg, while the upper part is richer in Al. Y and Nd, alloying elements of the substrate are present mainly in the lower part. Si, as an alloying element of the cladding powder is richer in the upper part and in the dark intermetallic particles (with similar composition than that shown for AZ61 and ZK30 alloys).

3.2. Microhardness testing

Microhardness testing measurements showed an important improvement in the hardness of the coatings as compared with Mg substrates. Figure 11 depicts the microhardness profile from the substrate to the coating surface for each material. In the coating zone, the hardness is not homogenous, showing two different areas corresponding with the lower and upper microstructure parts identified in the metallographic analysis. The lower area shows higher hardness (eutectic structure below the intermetallic band), range of 230-285 HV depending on the base alloy, than in the upper area, with hardness range of 140-170 HV. This effect is related with the eutectic microstructure and with the presence of hard intermetallic particles.

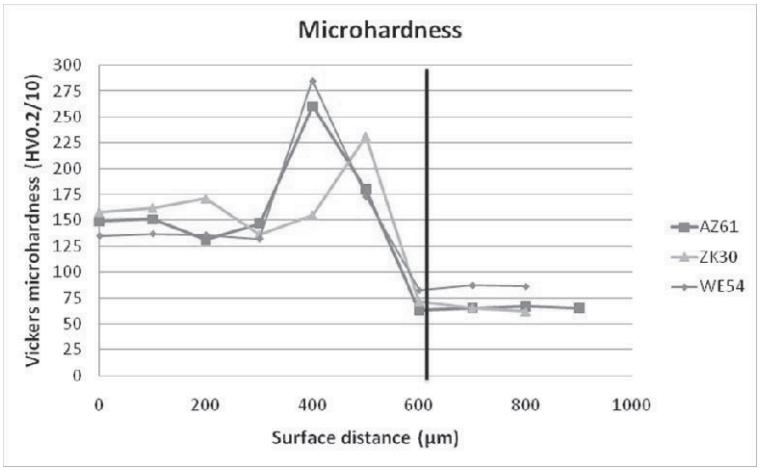

Figure 11. Microhardness profiles for AZ61, ZK30 and WE54 Mg alloys coated by laser cladding with Al-Si powder.

3.3. Salt Spray corrosion testing.

Corrosion was observed for all samples after the first 24 hours inside the SST chamber. Base material was in all cases more corroded than the coatings (figure 12), but anyway, the corrosion resistance was lower than expected for an aluminum coating. It is believed that the presence of magnesium in the coating, coming from the substrate by dilution with deposited material, affects negatively the corrosion resistance.

Another important aspect to notice is that the Mg substrates surrounding the Al-Si coatings were in all cases heavily corroded if compared with Mg substrates alone. This is attributed to galvanic corrosion, caused by the lower electrochemical corrosion potential of Mg compared to Al, thus making Mg act as a permanent sacrificial anode. In this way, if Al alloys coatings are applied on Mg substrates, the coating must cover the entire surface in order to avoid this negative galvanic effect.

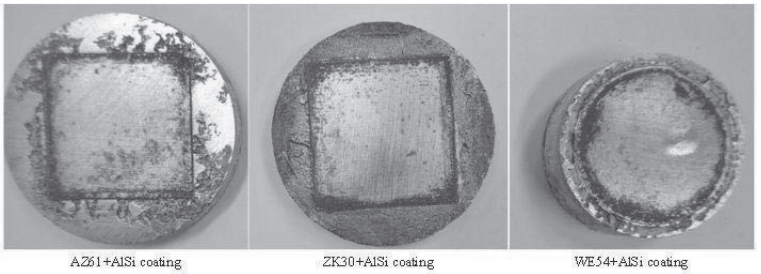

Figure.12 Laser cladding coated samples after salt spray testing (24h)

3.4. Sliding wear (pin on disc) testing.

3.4.1. Effect of the sliding distance on wear rates.

In contrast with results obtained by Yang et al. [5] for higher loads, in which volumetric wear rates increased with sliding length, current load configuration showed in all cases that the wear volumetric loss increases linearly with the sliding distance, giving as a result a constant volumetric wear rate (figure 13).

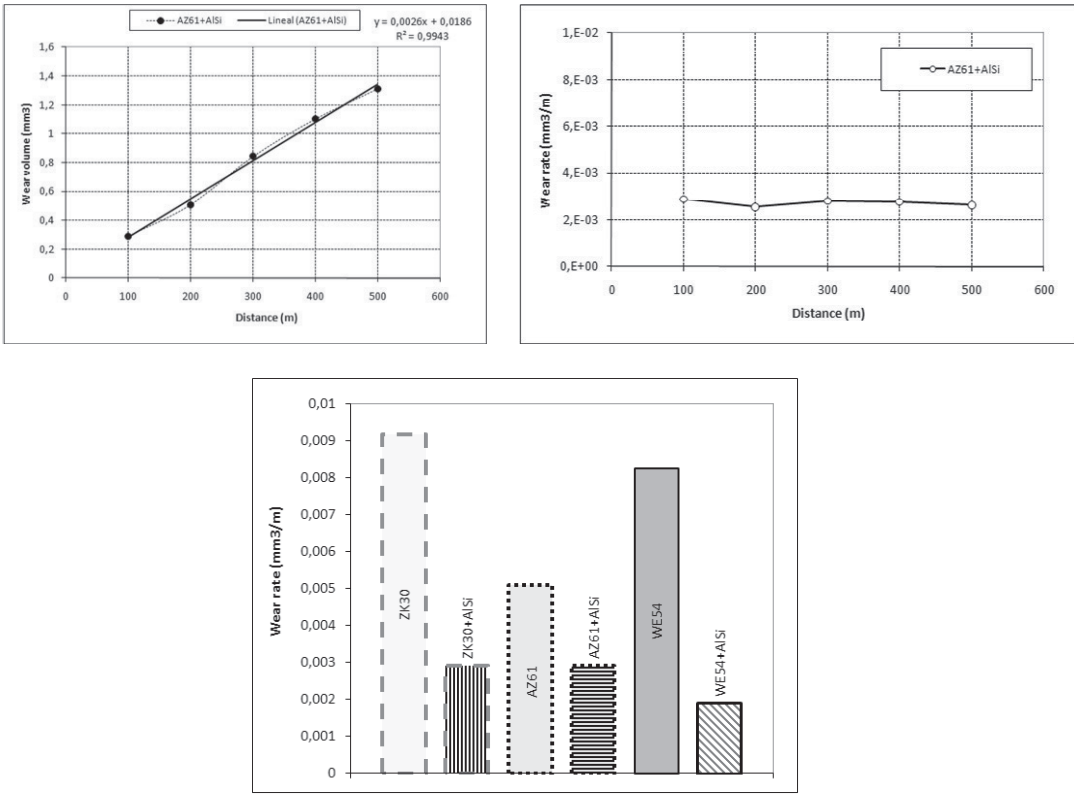

Figure 13. Left: Volume loss against sliding distance for Al-Si coating on AZ61 Mg. alloy. Right: Volume wear rate against sliding distance for Al-Si coating on AZ61 Mg. alloy. The wear rate is constant. This behavior is common for all samples.

3.4.2. Sliding wear rates.

Since measured wear rates were independent of testing distance, wear graphs have been constructed averaging the wear rate for the whole sliding distance (100-500m). Figure 14 shows wear rates for the whole set of experiments. The wear rate is, in all cases, higher for base magnesium alloys than for Al-Si coatings.

Figure 14. Averaged wear rates of Mg base materials and Al-Si laser cladding coatings.

3.4.3. Wear mechanisms.

Different wear mechanisms have been identified for base Mg materials and Al-Si laser cladding coatings. EDS analysis of Mg base alloys tracks showed strong oxygen peak in wear debris (figure 15). Oxygen value was 14.28%, much higher than 1.24 % detected for the base material. This behavior, previously observed by other authors [6], is referred as oxidation wear. Oxidation wear consist in the formation of oxidized chips (due to temperature increase during the sliding wear test), followed by the breakage of these brittle chips, generating abrasive oxidized debris.

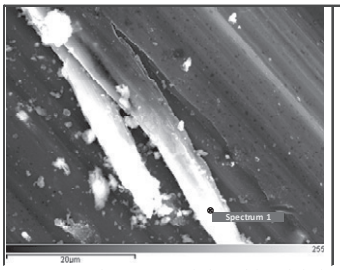

Element	Weight%	Atomic%
O K	14.28	21.34
Mg K	78.20	76.89
Y L	4.81	1.29
Ru L	0.56	0.13
Nd L	1.51	0.25
Gd L	0.29	0.04
Dy L	0.35	0.05
Totals	100.00	

Figure 15. Pin on disc wear debris on WE54 base material. White debris showing high oxygen content (oxidation).

For this loading configuration, the wear mechanism for Al-Si coatings is a combination of abrasive and adhesive wear, Although abrasive is the main mechanism, some adhesive zones are clearly visible (figure 16). As known, adhesive wear increases with load. In this way, it has been found that wear resistance of these coatings decreases for higher loads.

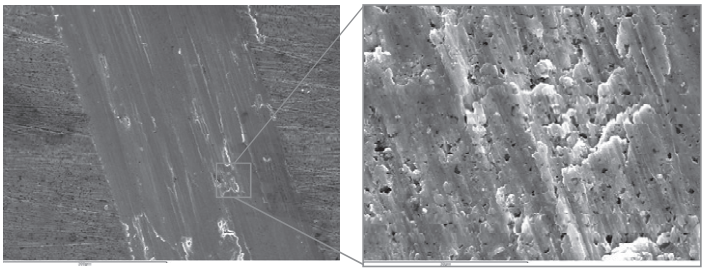

Figure 16. Pin on disc wear track on Al-Si coating (WE54 base) and detail of adhesive wear zone.

4. Conclusions

Laser cladding of Al12Si on Mg alloys (AZ61, ZK30 and WE54) have proven to be a suitable technique in order to obtain defect free coatings with higher hardness, corrosion resistance and wear resistance for low loading configuration.

Special care is required regarding the shielding athmosphere in order to avoid high plasma formation. Helium is preferable thanks to its high ionization potential.

Laser cladding Al-Si coatings showed heterogeneous microstructure, with two clearly diferentiable zones separated by a band of intermetallic particles. The lower zone, with eutectic microstructure and big intermetallic particles is the hardest area of the coating (230-285 HV), while for the upper zone the hardess is lower (140-170 HV), but significantly higher than for base Mg alloys (from 62HV for ZK30 to 88HV for WE54). The presence of this hardness gradient in the coating is undesirable, not improving the surface properties and making the coating more brittle and prone to internal cracking. The wear resistance of Al-Si coatings was, in all cases, better than for Mg base substrates. Abrasive wear was the governing mechanism, combined with some adhesive wear. Higher loads will increase the adhesive mechanism (for the same counter-part), making the coating less wear resistant.

Salt spray test showed that Al-Si coatings had better corrosion resistance than base Mg alloys, but not as good as expectable. Moreover Mg substrates in contact with Al based coatings suffered extreme galvanic corrosion, an important issue when designing Al coatings on Mg substrates.

Acknowledgements

The authors gratefully acknowledge the financial support by the Spanish ‘Centro de Desarrollo Tecnologico Industrial (CDTI)’ to the project ‘PROCESALI: Estudio de viabilidad y desarrollo tecnologico del procesado de componentes ligeros de magnesio y titanio para la ingeniería de transporte’ - Contract No.: IDI-20090370

References

[1] A.H. Wang, H.B. Xi, W.Y. Wang, Z.K. Bai, X.C. Zhu, C.S. Xie: YAG laser cladding of homogenous coating onto magnesium alloy. Materials Letters 60 (2006) 850–853
[2] B.J. Zheng, X.M.Chen, J.S.Lian: Microstructure and wear property of laser cladding Al+SiC powders on AZ91D magnesium alloy. Optics and Lasers in Engineering 48 (2010) 526–532
[3] Yao Jun, G.P. Sun, Hong-Ying Wang, S.Q. Jia, S.S. Jia: Laser (Nd:YAG) cladding of AZ91D magnesium alloys with Al + Si+Al2O3. Journal of Alloys and Compounds 407 (2006) 201–207
[4] X. Cao, M. Jahazi, J.P. Immarigeon, W. Wallace: A review of laser welding techniques for magnesium alloys. Journal of Materials Processing Technology 171 (2006) 188–204
[5] I. Yang, H. Wu. Improving the wear resistance of AZ91D magnesium alloy by laser cladding with Al-Si powders. Materials Letters 63 (2009) 19–21
[6] H. Chen, A.T. Alpas: Sliding wear map for the magnesium alloy Mg-9Al-0.9 Zn (AZ91). Wear 246 (2000) 106–116